Available online at www.sciencedirect.com
SCIENCE DIRECT®
Virology 322 (2004) 220–230
VIROLOGY
www.elsevier.com/locate/yviro

Morphological changes contribute to apoptotic cell death and are affected by caspase-3 and caspase-6 inhibitors during red sea bream iridovirus permissive replication

Masayuki Imajoh, Hidehiro Sugiura, and Syun-ichirou Oshima*

Fish Disease Laboratory, Department of Aquaculture, Kochi University, Nankoku, Kochi 783-8502, Japan

Received 5 November 2003; returned to author for revision 19 November 2003; accepted 4 February 2004

Abstract

Red sea bream iridovirus (RSIV) of the *Iridoviridae* family is a causative agent of lethal infections in many cultured marine fish species in southwestern Japan. RSIV-induced apoptosis was divided as follows: (1) cell shrinkage and rounding at the early apoptotic stage, (2) cell enlargement at the middle apoptotic stage, (3) formation of apoptotic body-like vesicles at the late apoptotic stage and phagocytosis by neighboring cells, and (4) loss of membrane integrity in apoptotic body-like vesicles without phagocytosis by neighboring cells. By affinity labeling, RSIV-induced apoptosis included caspase-dependent apoptosis. RSIV infection caused cell rounding but not cell enlargement or formation of apoptotic body-like vesicles and further restricted part of the structural protein synthesis in the presence of caspase-3 and -6 inhibitors. These findings showed the involvement of caspase-3 and -6 in the morphological changes at the middle and late apoptotic stages and viral protein synthesis in the late stage of RSIV infection.

Keywords: Red sea bream iridovirus; Apoptosis; Cytopathic effect; Affinity labeling; Active caspases; Caspase-3 inhibitor (Z-DEVD-FMK); Caspase-6 inhibitor (Z-VEID-FMK); Grunt fin cell line

Introduction

Iridoviruses are icosahedral cytoplasm DNA viruses that have been isolated from invertebrate and vertebrate host species. The *Iridoviridae* family includes four genera: *Iridovirus*, *Chloriridovirus*, *Ranavirus*, and *Lymphocystivirus* (Williams et al., 2000). Piscine iridoviruses have been classified as genera *Ranavirus* and *Lymphocystivirus*. Red sea bream iridovirus (RSIV) was first isolated as a causative agent of lethal infections from cultured red sea bream, *Pagrus major*, in Japan in 1992 and was defined as an unenveloped virus about 200–240 nm in diameter (Inouye et al., 1992). Infected fish have severe anemia and show petechia of the gills, congestion of the liver, and hypertrophy of the spleen and kidney. Based on the high homology of ATPase and major capsid protein (MCP) amino acid sequences, a new genus "Tropivirus" for five iridoviruses, including RSIV, from Southeast Asian countries has been proposed as the third piscine iridovirus in the family *Iridoviridae* (Sudthongkong et al., 2002).

Diagnostic procedures to isolate RSIV are often done by using the bluegill fry-2 (BF-2) cell line (Nakajima and Sorimachi, 1994, 1995; Oshima et al., 1998). A typical cytopathic effect (CPE) is characterized by cell rounding and enlargement in RSIV-infected BF-2 cells (Nakajima and Sorimachi, 1994). Morphological changes by viral infections contribute directly to CPE in the late stages of infection and resemble those of apoptosis (Collins, 1995). Among the *Iridoviridae* family, epizootic hematopoietic necrosis virus (EHNV), *Rana grylio* virus, and frog virus 3 (FV 3, type species of genus *Ranavirus*) belonging to the genus *Ranavirus* are known to induce apoptosis in fish cell lines (Chinchar et al., 2003; Essbauer and Ahne, 2002; Zhang et al., 2001). However, whether morphological changes by RSIV infection are due to induction of apoptosis in vitro is not understood.

Currently, it is clear that caspases (cysteine aspartate-specific proteases) play a central role in apoptosis. These proteases are synthesized as zymogen (or procaspase) and normally exist as an inactive form (Donepudi and Grutter, 2002). Many viral infections trigger alternative caspase signaling cascades initiated by either caspase-8 (death receptor-dependent apoptotic pathway) or caspase-9 (mitochondrion-dependent apoptotic pathway) (Everett and McFadden,

* Corresponding author. Fax: +81-88-864-5214.
E-mail address: S-Oshima@cc.kochi-u.ac.jp (S. Oshima).

0042-6822/$ - see front matter © 2004 Elsevier Inc. All rights reserved.
doi:10.1016/j.virol.2004.02.006

2001). Caspase-3, -6, and -7 are the downstream effector caspase in both death receptor-mediated and mitochondrion-dependent apoptosis whose activations cause the morphological changes in apoptosis (Enari et al., 1998; Thornberry and Lazebnik, 1998).

The RSIV disease has caused serious problems in marine aquaculture in southwestern Japan and has occurred in 31 cultured marine fish species from 1991 to 2000 (Kawakami and Nakajima, 2002). This disease has been also reported from different aquatic farms in Korea since 1998 and in Peng-hu Island on the southwest coast of Taiwan since 1993 (Jeong et al., 2003; Jung and Oh, 2000; Wang et al., 2003). Nevertheless, RSIV pathogenic mechanisms that lead to death are hardly understood both in vitro and in vivo.

In this study, a time course study of the development of morphological changes and apoptosis was done for RSIV-infected cells by monitoring using annexin V staining. To further understand how RSIV regulates apoptosis during viral infection, we also examined the morphological changes and viral protein synthesis in the presence of several caspase inhibitors.

Results

Time course kinetics of DNA fragmentation and viral growth in RSIV-infected GF cells

We firstly examined the ability of RSIV to induce DNA fragmentation in GF cells. As shown in Fig. 1A, a ladder pattern (200 bp) was first observed at 2 days after infection and continued to be observed up to 10 days after infection in RSIV-infected GF cells. As shown in Fig. 1B, the cell-associated and cell-free viral productions increased and were a maximum titer at 6 and 8 days after infection, respectively. After reaching the maximum titer, the cell-free viral production was maintained; however, the cell-associated viral production gradually decreased with continued incubation. Thus, the time course kinetics of DNA fragmentation and viral growth in RSIV-infected GF cells were parallel, indicating that viral replication and production of progeny virus are necessary to induce apoptosis in GF cells.

Morphological changes induced by RSIV infection in GF cells

Careful observation of RSIV-infected cells by light microscopy showed the sequential morphological changes (Fig. 2A) which were monitored by annexin V and propidium iodide (PI) staining (Fig. 2B) if the CPE by RSIV infection was due to apoptotic cell death. The first morphological change was cell shrinkage and rounding in RSIV-infected GF cells, which were occasionally observed throughout the entire monolayer at 2 days after infection. At 3 days after infection, enlarged cells appeared in part of the monolayer and were more frequent than rounded cells at 5 days after

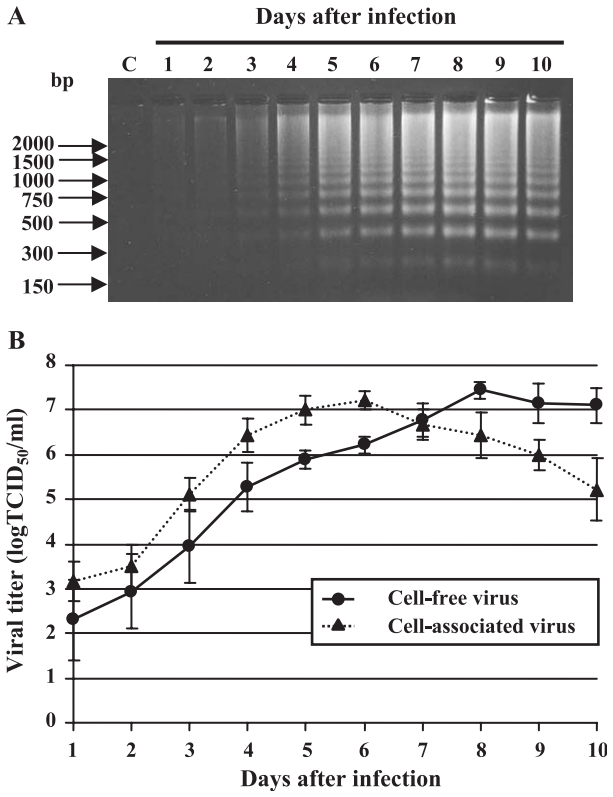

Fig. 1. Time course kinetics of DNA fragmentation (A) and viral growth (B) in RSIV-infected GF cells. (A) GF cells were either mock-infected or infected with the virus at a multiplicity of infection of 10 PFU per cell. At the indicated time after infection, low-molecular-weight DNA was extracted, precipitated, and analyzed by 2.0% agarose gel electrophoresis. Mock-infected cells were harvested at 10 days after infection (lane C). (B) GF cell monolayers were infected with the virus at a multiplicity of infection of 10 PFU per cell. At the indicated time after infection, cell-free and cell-associated viral concentrations were determined by $TCID_{50}$. All assays were analyzed in triplicate and error bars show standard deviation (SD).

infection. Both rounded and enlarged cells were stained with EGFP-annexin V. EGFP-annexin V-positive enlarged cells contained a condensed nucleus stained with PI, but other enlarged cells contained a swollen nucleus stained with PI. EGFP-annexin V-positive enlarged cells formed a membrane-bound vesicle containing a fragmented nucleus stained with PI at the plasma membrane, resulting in the remarkable appearance of apoptotic body-like vesicles at 7 days after infection. Both dye-positive vesicles probably gradually lost membrane integrity without phagocytosis by neighboring cells and were finally observed as vesicles apparently stained only with PI. This passive morphological change may be due to viral replication process and would not contribute to RSIV pathogenicity in vitro. The majority of attached cells were not finally observed at 10 days after infection.

Numerous numbers of both dye-positive enlarged cells and PI-positive vesicles

RSIV-infected GF cells were divided into six groups by the kind of dye and morphological characteristics of

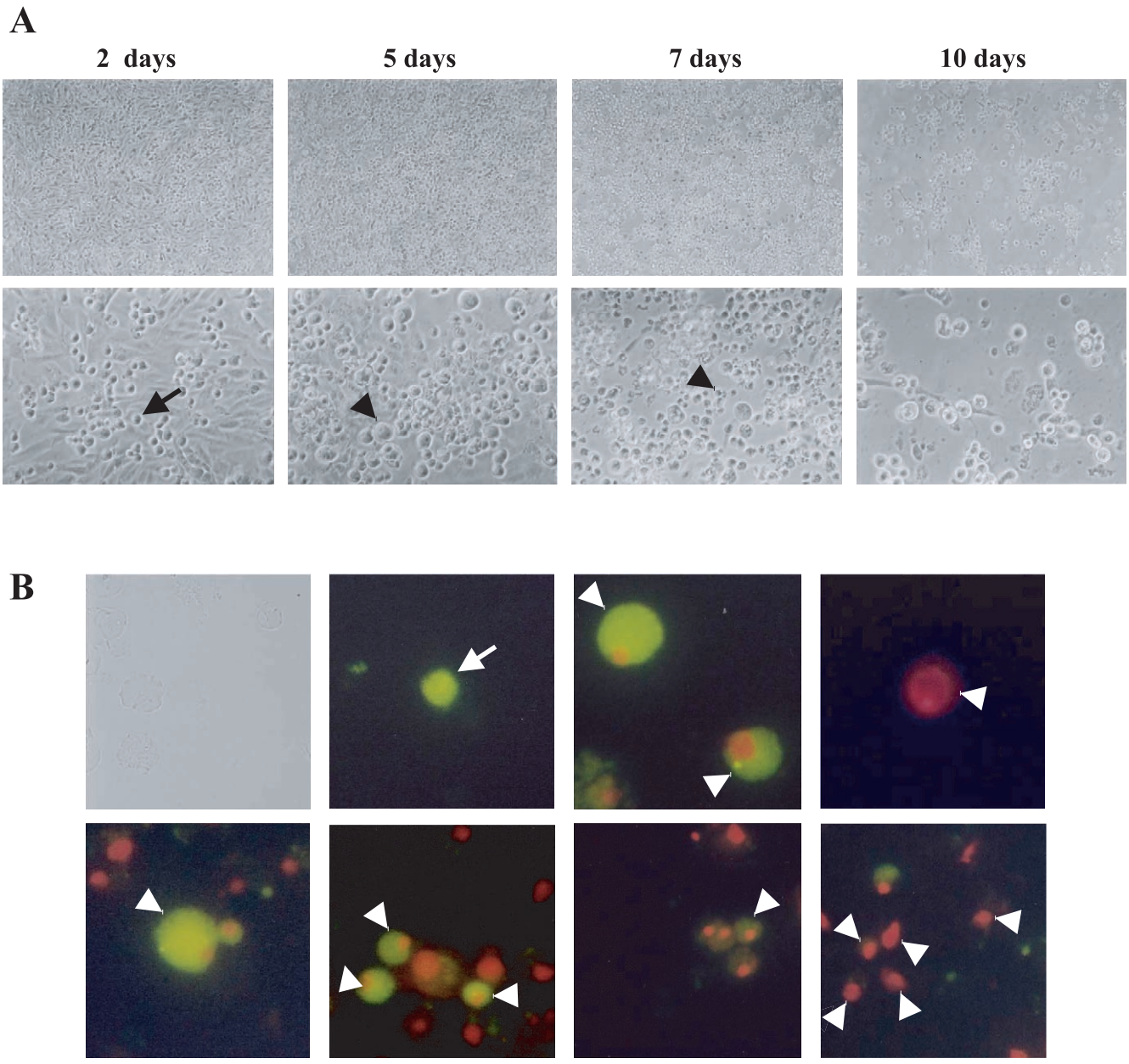

Fig. 2. Morphological changes in RSIV-infected GF cells. (A) CPE morphology at the indicated time after infection using light microscopy. At 2 days after infection, the rounded cells (indicated by long arrows) were observed throughout the entire monolayer. Enlarged cells (indicated by short arrows) were subsequently observed at 5 days after infection and then the majority of attached cells became apoptotic body-like vesicles (indicated by arrowheads) at 7 days after infection and detached from the cell dish up to 10 days after infection. Magnification: ×100 (upper panels) and ×300 (lower panels). (B) Fluorescent micrographs of the CPE by using annexin V and PI dyes. Normal cells were shown by light microscopy to compare the size with dye-stained cells. The long arrows indicated the rounded cells, short arrows indicated the enlarged cells, and arrowheads indicated the apoptotic like-vesicles, respectively. Magnification: ×1000.

cells, and 200 cells were counted four times in each group (Fig. 3). The number of EGFP-annexin V-positive rounded cells gradually increased and was 6.6 ± 0.8% (means ± SD) at 3 days after infection. Both dye-positive enlarged cells also increased and were the maximum number at 5 days after infection, more than EGFP-annexin V-positive rounded cells (30.9 ± 5.0%). After reaching the maximum number, the number of each kind of positive cell decreased by 10 days after infection. However, PI-positive enlarged cells kept low numbers even at 10 days after infection. PI-positive vesicles increased in number from 5 days after infection and had marked numbers from 8 to 10 days after infection. Compared with the number of PI-positive vesicles, EGFP-annexin V-positive and both dye-vesicles kept low numbers even at 10 days after infection. This tendency may be due to, for example, EGFP-annexin V-positive vesicles could not be counted when membrane integrity completely lost and both dye-positive vesicles faintly stained with EGFP-annexin V were not counted.

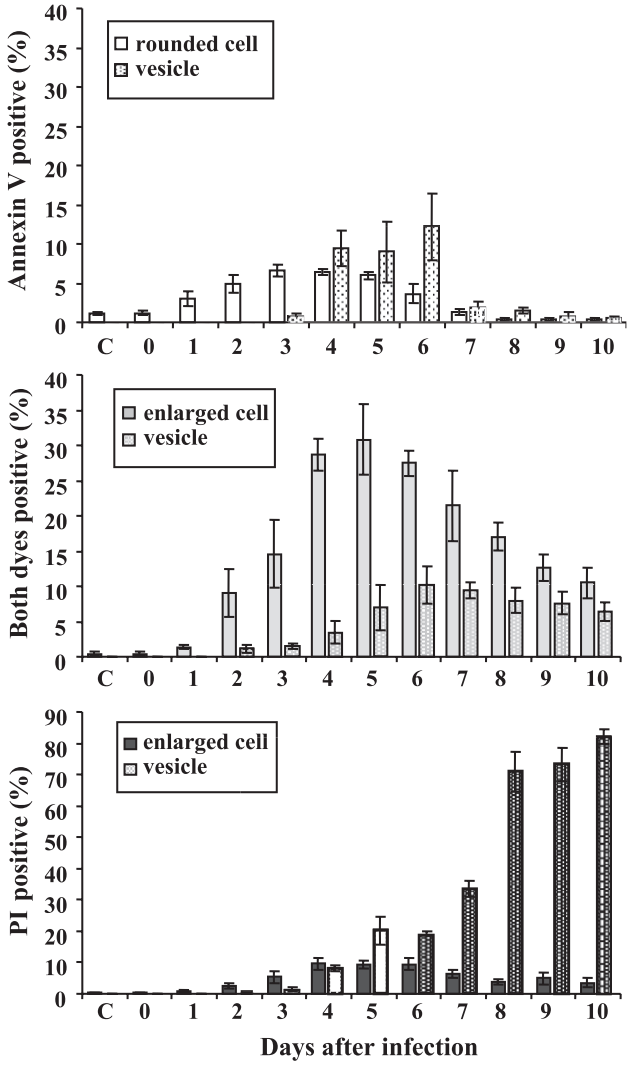

Fig. 3. The time course of morphologically changed cells with six different characteristics by RSIV infection. RSIV-infected GF cells could be divided into six groups by the kind of dyes and morphological characteristics of cells: (a) EGFP-annexin-positive rounded cell, (b) EGFP-annexin-positive vesicle, (c) both dye-positive enlarged cell, (d) both dye-positive vesicle, (e) PI-positive enlarged cell, (f) PI positive vesicle. Two-hundred cells were counted in each sample four times. Bars show standard deviation (SD).

Ultrastructural morphological changes by RSIV infection in GF cells

Fig. 4 shows the ultrastructure of RSIV-infected GF cells at 2 and 4 days after infection. At 2 days after infection, rounded cells showed vacuolization and chromatin condensation in the cytoplasm (Fig. 4A). At 4 days after infection, rounded cells were enlarged more than the cells shown in Fig. 4A because of increased cytoplasmic vacuolization (Fig. 4B). The enlarged cells contained a fragmented nucleus and many RSIV virions at distinct stages of development in its cytoplasm (Figs. 4C and D). RSIV virions were also in the cytoplasm of apoptotic body-like vesicles phagocytosed by neighboring GF cells (Figs. 4E and F).

Inhibition of caspase-3 and -6 activations affects morphological changes by RSIV infection in GF cells

Affinity labeling is useful to detect active caspases in apoptotic cells. This technique uses an irreversible biotin-labeled caspase inhibitor that covalently binds to large subunits of active caspases of approximately a molecular mass between 17 and 22 kDa (Eischen et al., 1997; Faleiro et al., 1997; Fearnhead et al., 1997; Martins et al., 1997, 1998). Between these molecular mass ranges, four major bands were detected as an active caspase candidate in RSIV-infected GF cells, but bands were undetectable in the nonproductive infections (Fig. 5A). These results showed that RSIV-induced apoptosis needed the activation of caspases during permissive replication. Although the active caspase bands had different patterns in RSIV-infected GF cells treated with caspase inhibitors, we failed to identify which caspase was involved in the four active caspase bands. However, at least, this result would represent that each caspase inhibitor selectively inactivated a specific caspase. To find further if RSIV-induced morphological changes need the activation of caspases, RSIV-infected GF cells treated with caspase inhibitors were carefully observed by light microscopy (Fig. 5B). At 5 days after infection, similar to RSIV-infected GF cells, enlarged cells and apoptotic body-like vesicles were frequently observed when RSIV-infected GF cells were treated with caspase-8 and -9 inhibitors. However, RSIV infection caused cell rounding, but not cell enlargement or formation of apoptotic body-like vesicles when RSIV-infected GF cells were treated with caspase-3, -6, and family inhibitors.

Inhibition of caspase-3 and -6 activations inhibits part of RSIV structural protein synthesis in GF cells

To confirm the viral structural protein synthesis in the treatment with caspase inhibitors or in the nonproductive infections, cell lysates were subjected to 12% SDS-polyacrylamide gels (Fig. 6A) and analyzed by using Western blot with anti-RSIV red sea bream serum (Fig. 6B). The SDS-PAGE profile in RSIV-infected GF cells resembled those in the treatment with caspase-8 and -9 inhibitors, but was different from those in the treatment with caspase-3, -6, and family inhibitors. Anti-RSIV red sea bream serum mainly reacted with three proteins with approximately molecular masses of 46, 22, and 19 kDa in RSIV-infected GF cells, which were similar to those of mouse serum antibody or monoclonal antibodies of previous studies (Nakajima and Sorimachi, 1995; Nakajima et al., 1998). These three bands were also detected when RSIV-infected GF cells were treated with caspase-8, -9, and family inhibitors, but the 19-kDa band was not detected when RSIV-infected GF cells were treated with caspase-3 and -6 inhibitors. The 46 and 22 kDa bands were faintly detected, but the 19-kDa band was not detected in heat-inactivated RSIV-infected GF cells. This result seemed to be because nonproductive RSIV virions bound to the cell surface but failed to enter the cytoplasm

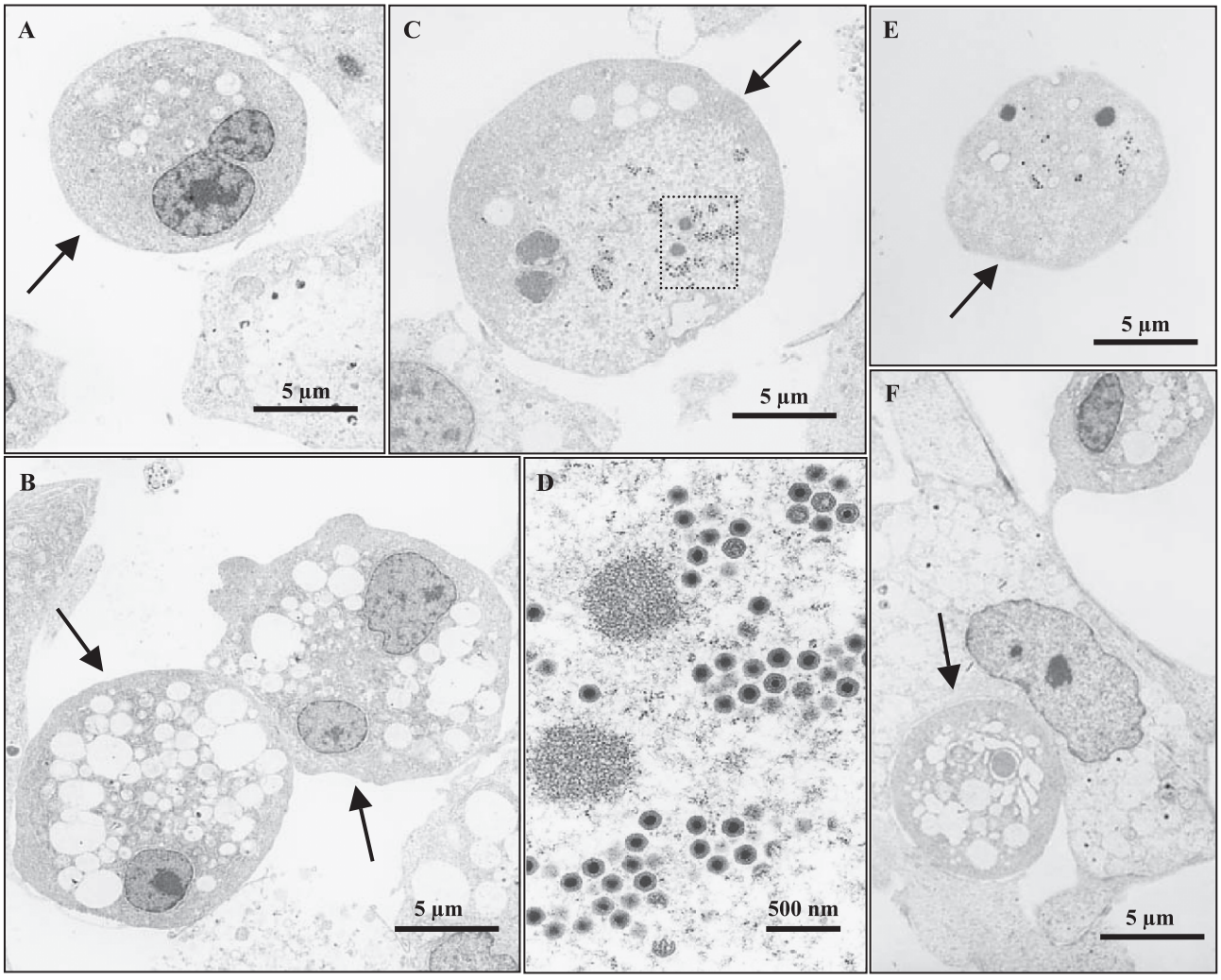

Fig. 4. Electron micrographs of RSIV-infected GF cells. Ultrathin sections were stained and were examined by using H-7100 Hitachi transmission electron microscopy. (A) Condensed nuclear fragmentation and cytoplasmic vacuolization in a shrunken and round cell, (B) fragmented nucleus and more vacuolization in enlarged cells, (C and D) RSIV virions in enlarged cell, (E and F) and apoptotic body-like vesicles contained RSIV virions and were phagocytosed by neighboring cell.

remained on the cell surface at a few detectable levels. Bands were undetectable when RSIV-infected GF cells were treated with PAA. Thus, RSIV replication was confirmed to be not complete in the nonproductive infections.

Discussion

In this study, we demonstrated that RSIV can induce apoptosis with common biochemical features such as DNA fragmentation of chromosomal DNA and PS translocation to the external layer in GF cells. These morphological changes by RSIV infection could be summarized in Fig. 7.

The development of CPE by RSIV infection seems to be unique among the *Iridoviridae* family. For example, in ranavirus infection, numerous small plaques first appear in the cell monolayer and then ranavirus-infected cells become rounded at the edge of the plaque, aggregate, and detach (Langdon et al., 1986; Qin et al., 2003; Zhang et al., 2001). Although cell enlargement by RSIV infection is a common morphological change in some fish cell lines, this mechanism has not been precisely understood. For CIV infection, enlarged cells are recognized as cell fusion and need the structural integrity of viral membrane (Cerutti and Devauchelle, 1979). CIV-infected cells lead rapidly to massive formation of syncytia that gradually become swollen and granular, and form vacuoles of various sizes, resulting in rounded cells that gradually detach. Our findings indicated at least that numerous enlarged cells corresponded to the middle apoptotic stage followed by the formation of membrane-bound vesicles at the cell membrane. Thus, progressive process of enlarged cells is obviously different between unenveloped RSIV and enveloped CIV infection.

RSIV infection caused cell rounding but not cell enlargement or formation of apoptotic body-like vesicles in the treatment with caspase-3 and -6 inhibitors. Caspase-3

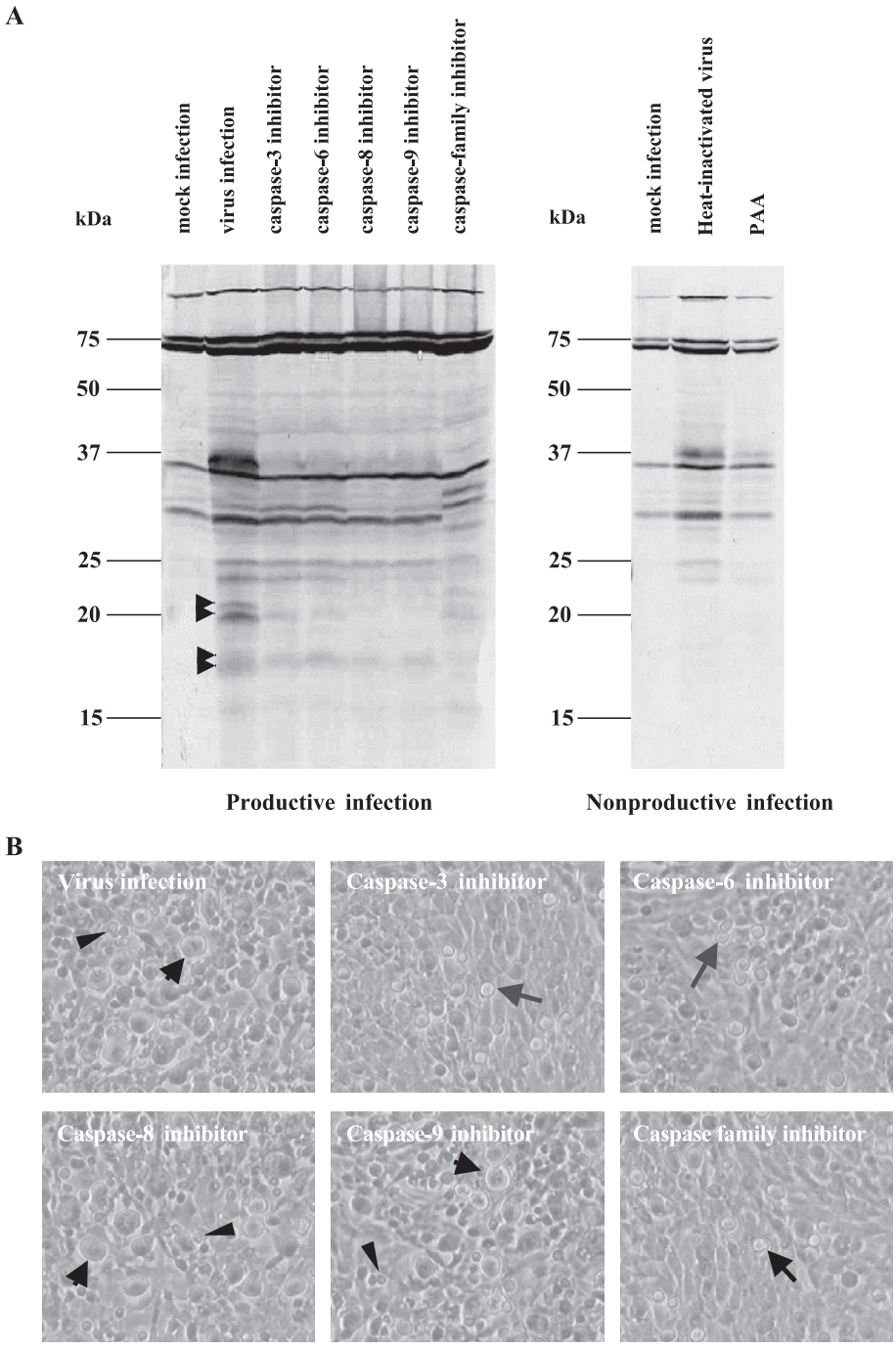

Fig. 5. (A) Affinity labeling of active caspases in RSIV-infected GF cells. Cell lysates were incubated with 1 μM Z-EK (bio) D-aomk, subjected to 16% SDS-polyacrylamide gel, and transferred electrophoretically onto PVDF membrane. Labeled caspases were visualized by using Amplified Alkaline Phosphatase Goat Anti-Rabbit Immun-Blot Assay Kit. Arrowheads indicate major bands as active caspase candidates. (B) Morphological changes in RSIV-infected GF cells in the treatment of caspase inhibitors. At 5 days after infection, enlarged cells and apoptotic body-like vesicles (short arrows and arrowhead, respectively) were often observed in RSIV-infected GF cells. Similar CPE was observed in the treatment with caspase-8 and -9 inhibitors. However, rounded cells (long arrows) were almost observed in the treatment with caspase-3, -6, and family inhibitors. Magnification: ×300.

has a major role in chromatin condensation, nuclear fragmentation, and the formation of apoptotic bodies (Hirata et al., 1998; Porter and Janicke, 1999). An amplification loop is downstream of the caspase cascade, where caspase-3 and -6 activate each other to amplify their activity (Kawahara et al., 1998; Xanthoudakis et al., 1999). Caspase-6 also induces nuclear and chromatin condensation and nuclear fragmentation by cleaving nuclear lamins (Orth et al., 1996; Takahashi et al., 1996). These roles of caspase-3 and -6 obviously coincide with

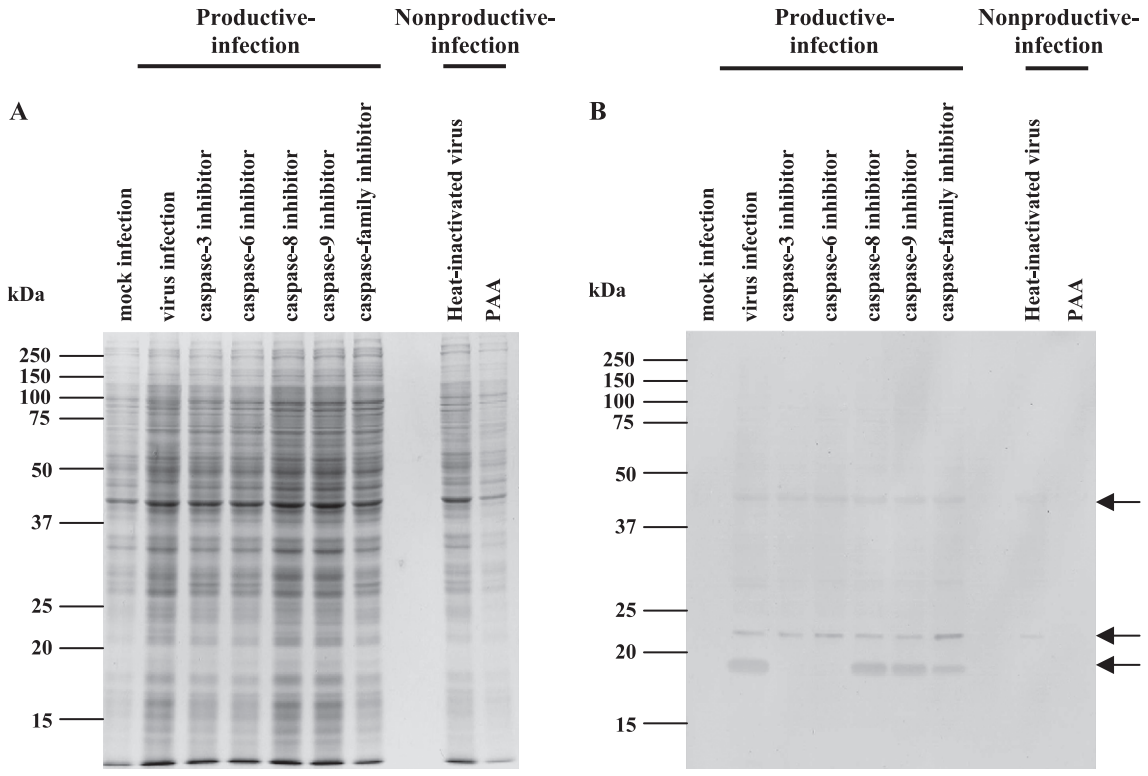

Fig. 6. Detection of RSIV protein analyzed by Western bloting. Cell lysate was separated by 12% SDS-polyacrylamide gel and transferred electrophoretically onto a nitrocellulose membrane. The gel was stained with Coomassie brilliant blue (A) and the membrane was processed for Western blot analysis (B). RSIV structural proteins were detected using experimentally RSIV-infected red sea bream serum at 1:200 dilution in PBS. The membrane was then incubated with anti-red sea bream IgM rabbit serum at 1:500 dilution and horseradish peroxidase (HRP)-conjugated goat anti-rabbit IgG at 1:2500 dilution in PBS. Color development was done using Konica Immunostaining HRP-1000 (Konica).

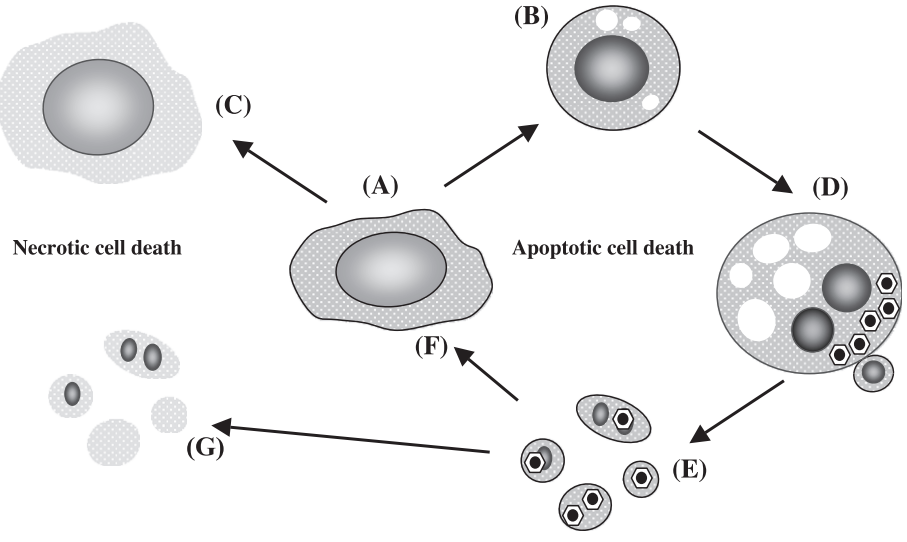

Fig. 7. Diagram illustrating the morphological changes and viral replications in RSIV-infected GF cells. (A) Normal cell. (B) RSIV-infected cell firstly showed cell rounding, cytoplasmic vacuolization, and chromatin condensation. RSIV-induced enlarged cells showed two distinct characteristics as follows. (C) One enlarged cell contained a swollen nucleus. (D) Another enlarged cell underwent severe morphological changes, such as increased cytoplasmic vacuolization, nuclear fragmentation, and formation of membrane-bound vesicle at the cell membrane. This enlarged cell contained many RSIV virions at distinct stages of development in its cytoplasm. (E and F) Apoptotic body-like vesicles were phagocytosed by neighboring cell. (G) Apoptotic body-like vesicles gradually lost its membrane integrity without phagocytosis by neighboring cell.

the biochemical changes of RSIV-induced apoptotic-enlarged cells observed by using fluorescence and electron microscopy. Interestingly, in addition to caspase-3 and -6 inhibitors, cell rounding was also observed when RSIV-infected GF cells were treated with caspase family inhibitor. In other viral infections, for example, caspase-3 activation by vesicular stomatitis virus infection is needed for efficient apoptosis induction but is not responsible for cell rounding (Hobbs et al., 2003). Cell rounding by coxsackievirus B3 infection is a caspase-independent morphological change (Carthy et al., 1998). Although the cellular factor of cell rounding has not been identified, our finding also indicates that caspases have no role in rounding RSIV-infected GF cells.

The SDS-PAGE profile proposed that viral protein synthesis was restricted in the treatment with caspase-3 and -6 inhibitors. In fact, anti-RSIV red sea bream serum reacted with 46-, 22-, and 19-kDa proteins in RSIV-infected GF cells and the 19-kDa band was not detected when RSIV-infected GF cells were treated with caspase-3 and -6 inhibitors. The 46-kDa protein is MCP that is similar in size to other iridoviruses (Chinchar et al., 1984; Davison et al., 1992; Hengstberger et al., 1993), but the properties of other proteins have not been characterized. The CIV gene expression cascade is primarily regulated at the transcriptional level that consists of mainly three different classes of immediate–early (IE), delayed–early (DE), and late (L) transcripts (Barray and Devauchelle, 1987). IE and DE transcripts are detected but L transcripts including the MCP gene are not detected when viral DNA synthesis is inhibited (D'Costa et al., 2001). Considering that the three structural proteins were undetectable in the treatment with PAA, we can regard that the 46-, 22-, and 19-kDa proteins were synthesized later in the RSIV infection. Taken together, we suggest that part of the L gene expression was restricted in the treatment of caspase-3 and -6 inhibitors.

Electron microscopy observation showed that the progeny virus spread to neighboring cells which phagocytosed apoptotic body-like vesicles after assembly of RSIV virions in enlarged cells. EHNV virions are released from the host cell membrane by budding and enter neighboring cells by endocytosis (Eaton et al., 1991). Alternatively, EHNV-induced apoptosis may not be important as a viral strategy to spread progeny viruses to neighboring cells. Further, FV3-induced apoptosis does not need viral gene expression (Chinchar et al., 2003). In such situation, host cellular defense mechanisms may induce premature apoptosis before viral replication maximizes and the progeny viruses spread to neighboring cells (Koyama et al., 2000). On the other hand, host cells may simultaneously permit a persistent infection if viruses have strategies to inhibit or at least delay host cell-induced premature apoptosis (O'Brien, 1998). RSIV-induced apoptosis needed the activation of caspases that were absent in the nonproductive infections. Therefore, RSIV permissive replication is an important process to induce caspase-dependent apoptosis, and apoptosis development directly relates to RSIV pathogenicity in vitro.

In this study, we provided the first evidence that RSIV induces caspase-dependent apoptosis during permissive replication. RSIV-induced apoptosis further showed the involvement of caspase-3 and -6 in the morphological changes at the middle and late apoptotic stages and viral protein synthesis in the late stage of RSIV infection. As the first appearance of RSIV virions in the cytoplasm of enlarged cells corresponded to the middle apoptotic stage, we can assume that caspase-3 and -6 inhibitors directly or indirectly affect part of the L gene expression and then the RSIV replication cycle is restricted before assembly of RSIV virions in rounded cells, resulting in reduced efficiency of RSIV replication. This idea needs more investigation and is an important clue to understand how the apoptotic signaling pathway is initiated by RSIV infection and how apoptotic cell death occurs during RSIV replication.

Materials and methods

Virus and cell

RSIV was originally isolated from RSIV-infected red sea bream in 2001 in Kochi, and the recloned virus in GF cells was used in this study. Although RSIV is efficiently isolated at a high titer in BF-2 cells, viral infectivity rapidly declines according to serial passage (Nakajima and Sorimachi, 1994). Thus, the GF cell line (Clem et al., 1961) is often used as an optical cell line to purify viruses and prepare vaccines (Kurita et al., 1998; Nakajima and Maeno, 1998; Nakajima et al., 1999, 2002). GF cells were cultured at 25 °C in Dulbecco's modified Eagle's medium nutrient mixture F-12 HAM (Sigma) supplemented with 10% fetal bovine serum (Hyclone) and 100 μg/ml kanamycin.

Virus infection

Viral infection was carried out with the virus at a multiplicity of infection of 10 PFU per cell for DNA fragmentation analysis, annexin V staining, electron microscopy, and virus 50% tissue culture infective doses ($TCID_{50}$).

DNA fragmentation analysis

Cells were seeded onto 24-well tissue culture plates and were incubated at 25 °C overnight. After viral infection, cells were harvested by centrifugation at 500 × *g* at 4 °C for 10 min. Cells were lysed with lysis buffer (10 mM Tris–HCl, pH 7.4, 10 mM EDTA, 0.5% Triton X-100) and the lysates were treated with RNase A (10 mg/ml) and then with proteinase K (20 mg/ml). DNA was precipitated in 0.5 M sodium chloride and 50% 2-propanol at −20 °C overnight, and then underwent 2.0% agarose gel electrophoresis.

Virus titer

Viral production was measured by using the $TCID_{50}$ method with GF cells grown in 96-well tissue culture plates. Both cell-free and cell-associated viral concentrations were measured. After viral infection, cell-free viruses were collected from the supernatant by centrifugation at 1400 × *g* at 4 °C for 10 min. The cells were resuspended in the medium and then cell-associated viruses were collected by freeze–thawing three times. All assays were analyzed in triplicate.

Monitoring of apoptotic and necrotic cells by annexin V and PI staining

Cells were seeded onto 24-well tissue culture plates and were incubated at 25 °C overnight. After viral infection, cells were harvested by centrifugation at 500 × *g* at 4 °C for 10 min. To detect PS distribution on the cell surface at early apoptosis, annexin V staining was done with annexin-V and PI by using an Annexin V-EGFP Apoptosis Detection Kit (MBL) according to the manufacturer's instructions. Microscopic fields were viewed by fluorescence microscopy and 200 cells were counted four times in each sample.

Transmission electron microscopy (TEM)

Cells were seeded onto a two-chamber slide and incubated at 25 °C overnight. The virus-infected cells were fixed with 1.5% glutaraldehyde for 10 min, washed three times with PBS, post-fixed with 1.0% osmium, and then dehydrated by serial concentrations of ethanol. The samples were embedded in epoxy resin and were cut into ultrathin sections by using an ultramicrotome. The ultrathin sections were placed on grids and were stained with uranyl acetate and lead citrate. The stained grids were observed by TEM (H-7100 Hitachi).

Cell lysate preparation

Cells were seeded in a 25 cm^2 tissue culture flask and incubated at 25 °C overnight. For affinity labeling of active caspases and Western blot analysis of viral protein synthesis, viral infection was done in three ways after productive infection with the virus at a multiplicity of infection of 10 PFU per cell and nonproductive infections with the virus at a multiplicity of infection of 10 PFU per cell in the presence of 200 μg/ml phosphonoacetic acid (PAA), an inhibitor of viral DNA synthesis, or with heat-inactivated virus (pretreatment at 56 °C for 30 min) at a multiplicity of infection of 10 PFU per cell. After centrifugation at 1000 × *g* at 4 °C for 10 min at 5 days after infection, cells were washed twice in PBS and resuspended in KPM buffer (50 mM KCl, 50 mM PIPES, 10 mM EGTA, 1.92 mM $MgCl_2$, pH 7.0, 1 mM dithiothreitol, 10 μg/ml cytochalasin B, 0.1 mM phenylmethylsulfonyl fluoride, 2 μg/ml pepstatin, 2 μg/ml leupeptin), and then by freeze–thawing five times in liquid nitrogen. After centrifugation at 9000 × *g* at 4 °C for 15 min, the cell lysates were stored at −80 °C until use.

Affinity labeling of active caspases and affinity blot analysis

Detection of active caspases in RSIV-infected GF cells was done by affinity labeling with Z-EK (bio) D-aomk (Peptide Institute, Inc). Cell lysates were incubated with 1 μM Z-EK (bio) D-aomk at room temperature for 1 h, mixed with 1× sample buffer (62.5 mM Tris–HCl, 2% SDS, 10% glycerol, 0.005% bromophenol blue, 5% 2-mercaptoethanol, pH 6.8), and boiled at 100 °C for 5 min.

Cell lysates (40 μg) labeled with Z-EK (bio) D-aomk were separated by electrophoresis on 16% SDS-polyacrylamide gels and transferred electrophoretically onto a polyvinylidene difluoride (PVDF) membrane (Bio-Rad). Color was developed by using Amplified Alkaline Phosphatase Goat Anti-Rabbit Immun-Blot Assay Kit (Bio-Rad) according to the manufacturer's instructions.

SDS-polyacrylamide gel electrophoresis and Western blot analysis

Cell lysates (20 μg) were separated by electrophoresis on 12% SDS-polyacrylamide gel and transferred electrophoretically onto a nitrocellulose membrane (Bio-Rad) for Western blot analysis. The membrane was blocked in PBS containing 5% skimmed milk. Viral proteins were detected in red sea bream serum experimentally infected with RSIV at a dilution of 1:200 in PBS. The membrane was then incubated with anti-red sea bream IgM rabbit serum at a dilution of 1:500 and horseradish peroxidase (HRP)-conjugated goat anti-rabbit IgG at a dilution of 1:2500 in PBS. After each reaction at room temperature for 1 h, the membrane was washed twice 0.05% Tween–PBS and then finally in PBS. Color development was done by using Konica Immunostaining HRP-1000 (Konica).

Caspase inhibition

Several caspase inhibitors, including caspase-3 inhibitor (Z-DEVD-FMK), caspase-6 inhibitor, (Z-VEID-FMK), caspase-8 inhibitor (Z-IETD-FMK), caspase-9 inhibitor (Z-LEHD-FMK), and caspase family inhibitor (Z-VAD (OMe)-FMK) (caspase-3, -6, -8, -9 inhibitor, BioVision; caspase family inhibitor, Enzyme Systems Products), were used. Cells were seeded in a 25 cm^2 tissue culture flask (Falcon) and incubated at 25 °C overnight. Each 20 μM caspase inhibitor was added to the culture medium. After replacing with fresh medium at 5 h after treatment, 20-μM caspase inhibitors were added once and the cells were infected with virus at a multiplicity of infection of 10 PFU per cell. Then at each 18 h after treatment, the medium was replaced with fresh medium and 20-μM caspase inhibitors were added. At 5 days after infection, the cell

lysates were analyzed by affinity blotting and Western blotting.

Acknowledgments

We are grateful to Dr. T. Taniguchi and Dr. K. Yagyu, Kochi Medical School, for their technical and scientific advice.

References

Barray, S., Devauchelle, G., 1987. Protein synthesis in cells infected by Chilo iridescent virus: evidence for temporal control of three classes of induced polypeptides. Ann. Inst. Pasteur/Virol. 138, 253–261.

Carthy, C.M., Granville, D.J., Watson, K.A., Anderson, D.R., Wilson, J.E. Yang, D., Hunt, D.W., McManus, B.M., 1998. Caspase activation and specific cleavage of substrates after coxsackievirus B3-induced cytopathic effect in HeLa cells. J. Virol. 72, 7669–7675.

Cerutti, M., Devauchelle, G., 1979. Cell fusion induced by invertebrate virus. Arch. Virol. 61, 149–155.

Chinchar, V.G., Metzger, D.W., Granoff, A., Goorha, R., 1984. Localization of frog virus 3 proteins using monoclonal antibodies. Virology 137, 211–216.

Chinchar, V.G., Bryan, L., Wang, J., Long, S., Chinchar, G.D., 2003. Induction of apoptosis in frog virus 3-infected cells. Virology 306, 303–312.

Clem, L.W., Moewus, L., Sigel, M.M., 1961. Studies with cells from marine fish in tissue culture. Proc. Soc. Exp. Biol. Med. 108, 762–766.

Collins, M., 1995. Potential roles of apoptosis in viral pathogenesis. Am. J. Respir. Crit. Care Med. 152, S20–S24.

Davison, S., Carne, A., McMillan, N.A.J., Kalmakoff, J., 1992. A comparison of the structural polypeptides of three iridescent viruses (types 6, 9, and 16) and the mapping of the DNA region coding for their major capsid polypeptides. Arch. Virol. 123, 229–237.

D'Costa, S.M., Yao, H., Bilimoria, S.L., 2001. Transcription and temporal cascade in Chilo iridescent virus infected cells. Arch. Virol. 146, 2165–2178.

Donepudi, M., Grutter, M.G., 2002. Structure and zymogen activation of caspases. Biophys. Chem. 101–102, 145–153.

Eaton, B.T., Hyatt, A.D., Hengstberger, S., 1991. Epizootic haematopoietic necrosis virus: purification and classification. J. Fish Dis. 14, 157–169.

Eischen, C.M., Kottke, T.J., Martins, L.M., Basi, G.S., Tung, J.S., Earnshaw, W.C., Leibson, P.J., Kaufmann, S.H., 1997. Comparison of apoptosis in wild-type and Fas-resistant cells: chemotherapy-induced apoptosis is not dependent on Fas/Fas ligand interactions. Blood 90, 935–943.

Enari, M., Sakahira, H., Yokoyama, H., 1998. A caspase-activated DNase that degrades DNA during apoptosis, and its inhibitor ICAD. Nature 391, 43–50.

Essbauer, S., Ahne, W., 2002. The epizootic haematopoietic necrosis virus (*Iridoviridae*) induces apoptosis in vitro. J. Vet. Med. B 49, 25–30.

Everett, H., McFadden, G., 2001. Viruses and apoptosis: meddling with mitochondria. Virology 288, 1–7.

Faleiro, L., Kobayashi, R., Fearnhead, H., Lazebnik, Y., 1997. Multiple species of CPP32 and Mch2 are the major active caspases present in apoptotic cells. EMBO J. 16, 2271–2281.

Fearnhead, H.O., McCurrach, M.E., O'Neill, J., Zhang, K., Lowe, S.W., Lazebnik, Y.A., 1997. Oncogene-dependent apoptosis in extracts from drug-resistant cells. Genes Dev. 11, 1266–1276.

Hengstberger, S.G., Hyatt, A.D., Speare, R., Coupar, B.E.H., 1993. Comparison of epizootic haematopoietic necrosis and Bohle iridoviruses, recently isolated Australian iridoviruses. Dis. Aquat. Org. 15, 93–107.

Hirata, H., Takahashi, A., Kobayashi, S., Yonehara, S., Sawai, H., Okazaki, T., Yamamoto, K., Sasada, M., 1998. Caspases are activated in a branched protease cascade and control distinct downstream processes in Fas-induced apoptosis. J. Exp. Med. 187, 587–600.

Hobbs, J.A., Hommel-Berrey, G., Brahmi, Z., 2003. Requirement of caspase-3 for efficient apoptosis induction and caspase-7 activation but not viral replication or cell rounding in cells infected with vesicular stomatitis virus. Hum. Immunol. 64, 82–92.

Inouye, K., Yamano, K., Maeno, Y., Nakajima, K., Matsuoka, M., Wada, Y., Sorimachi, M., 1992. Iridovirus infection of cultured red sea bream, *Pagrus major*. Fish Pathol. 27, 19–27.

Jeong, J.B., Jun, L.J., Yoo, M.H., Kim, M.S., Komisar, J.L., Jeong, H.D., 2003. Characterization of the DNA nucleotide sequences in the genome of red sea bream iridoviruses isolated in Korea. Aquaculture 220, 119–133.

Jung, S.J., Oh, M.J., 2000. Irudovirus-like infection associated with high mortalities of striped beakperch, *Oplegnathus fasciatus* (Temminck et Schlegel), in southern coastal areas of the Korean peninsula. J. Fish Dis. 23, 223–226.

Kawahara, A., Enari, M., Talanian, R.V., Wong, W.W., Nagata, S., 1998. Fas-induced DNA fragmentation and proteolysis of nuclear proteins. Genes Cells 3, 297–306.

Kawakami, H., Nakajima, K., 2002. Cultured fish species affected by red sea bream iridoviral disease from 1996 to 2000. Fish Pathol. 37, 45–47.

Koyama, A., Fukumori, T., Fujita, M., Irie, H., Adachi, A., 2000. Physiological significance of apoptosis in animal virus infection. Microbes Infect. 2, 1111–1117.

Kurita, J., Nakajima, K., Hirono, I., Aoki, T., 1998. Polymerase chain reaction (PCR) amplification of DNA of red sea bream iridovirus (RSIV). Fish Pathol. 33, 17–23.

Langdon, J.S., Humphrey, J.D., Williams, L.M., Hyatt, A.D., Westbury, H.A., 1986. First virus isolation from Australian fish: an iridovirus-like pathogen from redfin perch, *Perca fluviatilis* L. J. Fish Dis. 9, 263–268.

Martins, L.M., Kottke, T., Mesner, P.W., Basi, G.S., Sinha, S., Frigon Jr., N., Tatar, E., Tung, J.S., Bryant, K., Takahashi, A., Svingen, P.A., Madden, B.J., McCormick, D.J., Earnshaw, W.C., Kaufmann, S.H., 1997. Activation of multiple interleukin-1β converting enzyme homologues in cytosol and nuclei of HL-60 cells during etoposide-induced apoptosis. J. Biol. Chem. 272, 7421–7430.

Martins, L.M., Kottke, T.J., Kaufmann, S.H., Earnshaw, W.C., 1998. Phosphorylated forms of activated caspases are present in cytosol from HL-60 cells during etoposide-induced apoptosis. Blood 92, 3042–3049.

Nakajima, K., Sorimachi, M., 1994. Biological and physico-chemical properties of the iridovirus isolated from cultured red sea bream, *Pagrus major*. Fish Pathol. 29, 29–33.

Nakajima, K., Sorimachi, M., 1995. Production of monoclonal antibodies against red sea bream iridovirus. Fish Pathol. 30, 47–52.

Nakajima, K., Maeno, Y., 1998. Pathogenicity of red sea bream iridovirus and other fish iridoviruses to red sea bream. Fish Pathol. 33, 143–144.

Nakajima, K., Maeno, Y., Yokoyama, K., Kaji, C., Manabe, S., 1998. Antigen analysis of red sea bream iridovirus and comparison with other fish iridoviruses. Fish Pathol. 33, 73–78.

Nakajima, K., Maeno, Y., Honda, A., Yokoyama, K., Tooriyama, T., Menabe, S., 1999. Effectiveness of a vaccine against red sea bream iridoviral disease in a field trial test. Dis. Aquat. Org. 36, 73–75.

Nakajima, K., Ito, T., Kurita, J., Kawakami, H., Itano, T., Fukuda, Y., Aoi, T., Tooriyama, T., Manabe, S., 2002. Effectiveness of a vaccine against red sea bream iridoviral disease in various cultured marine fish under laboratory conditions. Fish Pathol. 37, 90–91.

O'Brien, V., 1998. Viruses and apoptosis. J. Gen. Virol. 79, 1833–1845.

Orth, K., Chinnaiyan, A.M., Garg, M., Froelich, C.J., Dixit, V.M., 1996. The CED-3/ICE-like protease Mch2 is activated during apoptosis and cleaves the death substrate lamin A. J. Biol. Chem. 271, 16443–16446.

Oshima, S., Hata, J.-I., Hirasawa, N., Ohtaka, T., Hirono, I., Aoki, T., Yamashita, S., 1998. Rapid diagnosis of red sea bream iridovirus infection using the polymerase chain reaction. Dis. Aquat. Org. 32, 87–90.

Porter, A.G., Janicke, R.U., 1999. Emerging roles of caspase-3 in apoptosis. Cell Death Differ. 6, 99–104.

Qin, Q.W., Chang, S.F., Ngoh-Lim, G.H., Gibson-Kueh, S., Shi, C., Lam, T.J., 2003. Characterization of a novel ranavirus isolated from grouper *Epinephelus tauvina*. Dis. Aquat. Org. 53, 1–9.

Sudthongkong, C., Miyata, M., Miyazaki, T., 2002. Viral DNA sequences of genes encoding the ATPase and the major capsid protein of tropical iridovirus isolates which are pathogenic to fishes in Japan, South China Sea and Southeast Asian countries. Arch. Virol. 147, 2089–2109.

Takahashi, A., Alnemri, E.S., Lazebnik, Y.A., Fernandes-Alnemri, T., Litwack, G., Moir, R.D., Goldman, R.D., Poirier, G.G., Kaufmann, S.H., Earnshaw, W.C., 1996. Cleavage of lamin A by Mch2 alpha but not CPP32: multiple interleukin 1 beta-converting enzyme-related proteases with distinct substrate recognition properties are active in apoptosis. Proc. Natl. Acad. Sci. U.S.A. 93, 8395–8400.

Thornberry, N.A., Lazebnik, Y., 1998. Caspases: enemies within. Science 281, 1312–1316.

Wang, C.S., Shih, H.H., Ku, C.C., Chen, S.N., 2003. Studies on epizootic iridovirus infection among red sea bream, *Pagrus major* (Temminck-Schlegel), cultured in Taiwan. J. Fish Dis. 26, 127–133.

Williams, T., Chinchar, G.D., Darai, G., Hyatt, A.D., Kalmakoff, J., Seligy, V.L., 2000. Family *Iridoviridae*. In: van Regenmortel, M.H.V., Fauquet, C.M., Bishop, D.H.L., Carstens, E.B., Estes, M.K., Lemon, S.M., Manniloff, J., Mayo, M.A., McGeoch, D.J., Pringle, C.R., Wickner, R.B. (Eds.), Virus Taxonomy. Seventh Report of the International Committee on Taxonomy of Viruses. Academic Press, San Diego, pp. 167–182.

Xanthoudakis, S., Roy, S., Rasper, D., Hennessey, T., Aubin, Y., Cassady, R., Tawa, P., Ruel, R., Rosen, A., Nicholson, D.W., 1999. Hsp60 accelerates the maturation of pro-caspase-3 by upstream activator proteases during apoptosis. EMBO J. 18, 2049–2056.

Zhang, Q.-Y., Xiao, F., Li, Z.-Q., Gui, J.-F., Mao, J., Chinchar, V.G., 2001. Characterization of an iridovirus from the cultured pig frog *Rana grylio* with lethal syndrome. Dis. Aquat. Org. 48, 27–36.